


*etc*  
APPLICATION OF THE METHODS OF LIMIT ANALYSIS  
TO THE EVALUATION OF THE STRENGTH  
OF FIBER-REINFORCED COMPOSITES

1. *MASW-1371*

by

L. S. Shu and B. W. Rosen

*27421*

FACILITY FORM 602	N 67 - 	(THRU)
	38	1
	CR84450	32
	(PAGES)	(CODE)
	(NASA CR OR TMX OR AD NUMBER)	(CATEGORY)

*2.*

January, 1967

GPO PRICE \$ \_\_\_\_\_

CFSTI PRICE(S) \$ \_\_\_\_\_

Hard copy (HC) *\$ 3.00*

Microfiche (MF) *.65*

*3. GPO, Technical*

ff 653 July 85

Space Sciences Laboratory  
General Electric Company  
Missile and Space Division  
Philadelphia, Pennsylvania 19101

## ACKNOWLEDGEMENT

The authors acknowledge the support under  
Contract NASw-1377 of the National Aeronautics and  
Space Administration during the performance of the work  
presented herein.

## SUMMARY

The in-plane shear strength and the transverse strength in shear and in tension of composites comprised of elastic-brittle fibers and an elastic perfectly plastic binder are evaluated quantitatively in terms of the matrix yield strength and volume fraction. The results are in the form of bounds obtained by the application of the theorems of limit analysis of plasticity.

### 1. INTRODUCTION

An important goal in the study of the mechanics of composite media is the determination of a theoretical relationship between the strength of a uniaxial fibrous composite and the mechanical properties and geometry of its constituents. A relationship of this type could be utilized both in the definition of desirable improvements in constituent properties as well as in the assessment of the structural potential of various composite materials.

The tensile and compressive strength of fibrous composites loaded parallel to the fibers has been studied by Rosen [1]\*. Transverse strength was studied by Hashin [2] using theorems of limit analysis of plasticity [3, 4]. Upper and lower bounds for limit loads were obtained under certain geometrical restrictions - namely, for those cases in which it is possible to put a plane through the fiber-reinforced body under consideration without cutting through any fibers. This prerequisite geometrical restriction is severe and it is the purpose of the present paper to obtain bounds of the limit loads without imposing this constraint.

---

\* Numbers in square brackets refer to Bibliography at the end of this paper.

## 2. STATEMENT OF THE PROBLEM

The present analysis considers a composite body with unidirectional circular reinforcing fibers of various diameters embedded in the matrix material. It is assumed that the fibers are elastic-brittle and that the matrix is elastic-perfectly plastic and obeys the von Mises' yield criterion. The body is subject to various simple surface tractions and it is desired to find the limit load for each set of surface tractions. This is defined as that load at which the deformation of the body can increase without any increase in load. In the present work, this load is defined as the failure load of the composite body and it is estimated by bounding it from above and below by the application of the methods of limit analysis of plasticity.

For convenience of analysis, the fiber-reinforced composite body under investigation is chosen to be a cylindrical specimen with

rectangular cross-section. The specimen is referred to an orthogonal Cartesian coordinate system whose  $x_1$ -axis is parallel to the reinforcing fibers which extend from base to base of the specimen as shown in Figure 1. Following Hashin and Rosen [5], the entire composite specimen is considered as an assemblage of composite cylinders. All fibers are surrounded entirely by concentric cylinders of matrix material in such a way that they are not overlapping. The cylinder consisting of a fiber of radius  $r_f$  and the outer matrix-shell of radius  $r_b$  is called a composite cylinder. It is assumed that the lateral surface of the specimen does not cut through any of the composite cylinders. The entire composite body is thus considered as an aggregate of the composite cylinders plus the remaining matrix-volume. Thus, if  $V$ ,  $V_1$  and  $V_2$  denote, respectively, the total volumes of the specimen, the composite cylinders and the remaining matrix in the specimen, the following obvious relation holds

$$V = V_1 + V_2 \quad (1)$$

In general,  $\beta \equiv \frac{r_f}{r_b}$  varies from one composite cylinder to another in a specimen and  $V_2 \neq 0$ . An idealized type of assemblage where  $\beta$  is the same for all composite cylinders (although the fibers are of different diameters) and  $V_2 = 0$  is called a "random array" [5].

### 3. LIMIT ANALYSIS OF THE COMPOSITE SPECIMEN

The von Mises' yield criterion which the matrix material is assumed to obey has the following form\* :

$$\frac{s_{ij} s_{ij}}{2} \leq k^2 \quad (2)$$

where  $s_{ij}$  are components of the stress deviator and  $k$  is the yield stress in simple shear for the matrix. Under the conditions of plane

---

\*Henceforth, unless otherwise specified,  $i, j = 1, 2, 3$ ; summation on repeated indices is implied.

strain perpendicular to  $x_1$ -axis, von Mises' yield criterion (2) reduces to

$$(\tau_{22} - \tau_{33})^2 + 4 \tau_{23}^2 \leq 4 k^2 \quad (3)$$

where  $\tau_{22}$ ,  $\tau_{33}$ , and  $\tau_{23}$  are components of the stress tensor in the transverse plane.

For practical composite materials, the fiber modulus is much higher than that of the matrix. Therefore, the fibers may be considered to be rigid.

The upper and lower bound theorems of limit analysis of plasticity will be used to obtain upper and lower bounds of the limit load. Readers are referred to [3, 4] for proofs of the theorems.

The surface tractions applied to the entire boundary surface  $S$  of the specimen can be described generally by the following relations:

$$T_i(S) = \tau_{ij} n_j \quad (4)$$

where  $T_i(S)$  are components of the surface tractions;  $\tau_{ij}$  are components of the stress tensor and  $n_j$  are components of the unit outward normal to  $S$ .



The following cases of surface loadings are considered:

Case 1. The surface tractions in (4) are such that  $\tau_{ij}$  has the following

form:

$$\tau_{ij} = \begin{bmatrix} 0 & \tau_{12} & 0 \\ \tau_{12} & 0 & 0 \\ 0 & 0 & 0 \end{bmatrix} \quad (5)$$

where  $\tau_{12}$  is a constant. This amounts to a uniform shear stress  $\tau_{12}$  applied on the boundary of the specimen as depicted diagrammatically in Figure 2 in the  $x_1 x_2$  plane.

According to the lower bound theorem, a lower bound of the limit load for the surface tractions  $T_i(S)$  is that load for which a statically admissible stress field exists in the body under consideration.

In this case, a uniform stress field

$$\tau_{ij} = \begin{bmatrix} 0 & \tau_0 & 0 \\ \tau_0 & 0 & 0 \\ 0 & 0 & 0 \end{bmatrix}$$

is chosen as a statically admissible stress field where  $\tau_0$  is such that

(2) is nowhere violated in the matrix. Then it can easily be shown that

the lower bound of the limit load of  $\tau_{12}$  is given by:

$$\left(\tau_{12}^L\right)_L = k \quad (6)$$

For upper bound construction, a kinematically admissible velocity field is chosen as follows:

(a) In the region of the composite specimen not occupied by the composite cylinders,

$$u_1 = 0, u_2 = \gamma_1 x_1, u_3 = 0 \quad (7)$$

where  $\gamma_1$  is any real number.

(b) In any composite cylinder, the velocity field  $u$  is the elastic displacement solution to the displacement boundary value problem with boundary conditions (7) prescribed. This result is obtained from Appendix 2 of [5] with the modification that the fibrous core is rigid.

For this velocity field, an upper bound of the limit load  $\tau_{12}^L$  can be obtained from the following expression:

$$\left(\tau_{12}^L\right)_U = \frac{\int_V F(\dot{\epsilon}_{ij}) dV}{V\gamma_1}$$

where  $F(\dot{\epsilon}_{ij})$ , to be integrated over the entire volume of the specimen, is the dissipation density function calculated from this kinematically admissible velocity field. For the general case where composite cylinders have different  $\beta$ 's, this yields:

$$\left(\frac{\tau_{12}^L}{k}\right)_U = 1 - \frac{V_1}{V} + \frac{1}{V} \sum_{i=1}^N V_c^{(i)} \left[ \frac{1}{\pi(1-\beta_i^2)} \int_{\beta_i}^1 \int_0^{2\pi} R \sqrt{\left(\frac{1+\beta_i^4}{R^4}\right) + 2\frac{\beta_i^2}{R^2} \cos \theta} d\theta dR \right] \quad (8)$$

where  $V_c^{(i)}$  is the total volume of the  $i^{\text{th}}$  composite cylinder;

$\beta_i$  is the ratio  $\frac{r_f}{r_b}$  for the  $i^{\text{th}}$  composite cylinder and  $N$  is the total

number of composite cylinders in the specimen.

In particular, for the case where all composite cylinders have the same  $\beta$ , (8) reduces to simple form

$$\left(\frac{\tau_{12}^L}{k}\right)_U = 1 + v_1 (I_1 - 1) \quad (9)$$

where

$$v_1 = \frac{V_1}{V}$$

and

$$I_1 = \frac{1}{\pi(1-\beta^2)} \int_{\beta}^1 \int_0^{2\pi} R \sqrt{\left(1 + \frac{\beta^4}{R^4}\right) + 2 \frac{\beta^2}{R^2} \cos \theta} d\theta dR \quad (10)$$

Further, in the case of the "random array" ( $V_2 = 0$ ), the fiber-volume fraction of the composite specimen,  $v_f = \beta^2$  and (9) becomes

$$\left(\frac{\tau_{12}^L}{k}\right)_U = I_1 \quad (11)$$

The integral  $I_1$  in (10) is integrated numerically for different  $\beta$ 's. The result is shown in Figure 3 where  $\left(\frac{\tau_{12}^L}{k}\right)_U$  in (11) is plotted as a function of  $v_f$  ( $0 < v_f < 1$ ,  $v_f = \beta^2$ ).

Notice particularly in Figure 3,

$$\lim_{v_f \rightarrow 0} \left(\frac{\tau_{12}^L}{k}\right)_U = 1$$

and

$$\lim_{v_f \rightarrow 1} \left(\frac{\tau_{12}^L}{k}\right)_U = \frac{4}{\pi}$$

From the above result, it is concluded that under the type of surface tractions described by (4) and (5), the strength of the matrix can be increased at most by about 27% due to fiber-reinforcement.

Another kinematically admissible velocity field can be constructed to obtain an upper bound  $\left(\frac{\tau_{12}^L}{k}\right)_U$  if the detailed geometry of array of fibers in a specimen is known. Construct a surface whose generator is

parallel to  $x_1$  - axis in such a way that the surface does not cut through any fibers. This can always be done due to the geometry of the composite specimen under consideration. A typical "cut" is shown in Figure 4. The kinematically admissible velocity field is defined by a constant velocity  $u$  in the positive  $x_1$ -direction of the portion of the specimen to the right of the "cut" relative to the rest of the specimen.

An application of the upper bound theorem gives

$$\frac{\left(\tau_{12}^L\right)_U}{k} = \frac{l_3}{\ell_3} \quad (12)$$

where  $\ell_3$  is the linear dimension of the specimen in  $x_3$ -direction and  $l_3$  is the total length of the curve which is the trace of the "cut" in the  $x_2 x_3$  plane.

Therefore, it is possible to construct an infinite number of different cuts to obtain different kinematically admissible velocity fields. The lowest upper bound  $\left(\tau_{12}^L\right)_U$  can be obtained from (12) by choosing the cut with the smallest  $l_3$ . This scheme is possible if the arrangement of fibers is known. For example, in the case of a "square array" of fibers in a specimen shown in Figure 5, it is always possible to choose a cut such that  $l_3 = \ell_3$  without cutting through any fibers regardless of fiber volume fractions of the specimen. Then  $\left(\tau_{12}^L\right)_U$  coincides with  $\left(\tau_{12}^L\right)_L$  which is  $k$ . Therefore, in the case of "square array", under the type of surface tractions considered, the presence of fiber-reinforcement does not help strengthening the matrix.

A more general situation exists in which the detailed geometry of the arrangement of fibers is not known but it is possible to obtain an upper bound for  $\tau_{12}^L$  by an application of (12). However, due to the fact that the detailed geometry is unknown, the upper bound obtained may not be the lowest for any given fiber-volume fraction. The geometry treated is that of circular fibers of different diameters embedded in an arbitrary manner in a matrix material to form a uni-directional fibrous composite cylindrical specimen of rectangular cross section as shown in  $x_2 x_3$  plane in Fig. 6. For any  $x_2$  in the specimen, a "cut" can be constructed as shown in Fig. 6. Thus,  $\lambda_3$  (in (12) ) associated with the "cut" is a function of  $x_2$ . More explicitly,

$$\lambda_3 = \ell_3 + (F-1) \ell_f$$

where  $\ell_f$  is the total length of the straight line segments within the fibers that a "cut" at  $x_2$  bypasses (as represented by dotted line segments in Fig. 6).  $F\ell_f$  is the total minimum arc length of the "cut" to replace  $\ell_f$  in order to avoid cutting the fibers. Obviously both  $\ell_f$  and  $F$  are functions of  $x_2$ , and

$$1 \leq F \leq \frac{\pi}{2}$$

Therefore, we seek the minimum value of  $\ell_f$ , defined by  $(\ell_f)_{\min}$ . Then the associated  $\lambda_3$ , denoted  $\lambda_3^0$ , can be bounded from above in the following manner:

$$\lambda_3^0 \leq l_3 + \left(\frac{\pi}{2} - 1\right) (l_f)_{\min.}$$

Further, since  $v_f$  is the mean volume fraction,

$$\frac{(l_f)_{\min.}}{l_3} \leq v_f$$

Combining the last two inequalities, we have

$$\lambda_3^0 \leq l_3 \left[ 1 + \left(\frac{\pi}{2} - 1\right) v_f \right]$$

Then by (12), we obtain an upper bound for  $\tau_{12}^L$ ,

$$\left(\frac{\tau_{12}^L}{k}\right)_U = 1 + \left(\frac{\pi}{2} - 1\right) v_f$$

The upper bound obtained above is a linear function of the fiber-volume fraction  $v_f$  ( $0 \leq v_f < 1$ ) for arbitrary arrangement of fibers in the matrix.

Case 2. Under the conditions of plane strain, the surface tractions in (4) are such that  $\tau_{ij}$  has the following form:

$$\tau_{ij} = \begin{bmatrix} 0 & 0 & 0 \\ 0 & 0 & \tau_{23} \\ 0 & \tau_{23} & 0 \end{bmatrix} \quad (13)$$

where  $\tau_{23}$  is a constant.

This amounts to uniform shear stresses  $\tau_{23}$  applied on the lateral boundary of the specimen as depicted diagrammatically in Fig. 7.

For lower bound construction, a uniform stress field

$$\tau_{ij} = \begin{bmatrix} 0 & 0 & 0 \\ 0 & 0 & \tau_o \\ 0 & \tau_o & 0 \end{bmatrix}$$

is chosen as a statically admissible stress field where  $\tau_o$  is such that (3) is nowhere violated in the matrix. Then it follows that the lower bound for the limit load

$$\left( \tau_{23}^L \right)_L = k \tag{14}$$

which is again independent of fiber volume fraction as shown in Figure 8.

It can be shown from the definition of a statically admissible stress field that  $k$  is the highest possible lower bound for  $\tau_{23}^L$  that can be obtained. Indeed, consider a most general statically admissible stress field  $\tau_{ij}^*$  in equilibrium with the boundary traction. As  $\tau_{23}$  increases monotonically,  $\tau_{ij}^*$  will also increase monotonically. The highest lower bound  $\left( \tau_{23}^L \right)_L$  for  $\tau_{23}^L$  is the value of  $\tau_{23}$  at which at some point of the matrix region in the specimen, the von Mises' yield criterion (3) is about to be violated. If the point is on the boundary of the specimen, then from (3) it is clear that  $\left( \tau_{23}^L \right)_L \leq k$ . If it is in the specimen, then  $\left( \tau_{23}^L \right)_L < k$ . Therefore, in the case where no fibers are cut by the lateral boundary surface of the specimen, which is consistent with the composite-cylinder-assembly model stated in Section 2,  $\left( \tau_{23}^L \right)_L$  cannot be higher than  $k$ . In cases where



lateral boundary surface consists of both fibers and matrix, a higher  $\left(\tau_{23}^L\right)_L$  might be obtained by considering the surface tractions being applied non-uniformly on the boundary. However, quantitative results have not yet been obtained.

For upper bound construction, the same principle as used in Case 1 is used here. A kinematically admissible velocity field is chosen as follows:

(a) In the region of the composite specimen not occupied by composite cylinders and on the boundary of the composite cylinders,

$$u_1 = 0, u_2 = \frac{\gamma_2}{2} x_3, u_3 = \frac{\gamma_2}{2} x_2 \quad (15)$$

where  $\gamma_2$  is any real number.

(b) In any composite cylinder, the velocity field  $\underline{u}(x_2, x_3)$  is the elastic displacement solution to the displacement boundary value problem with displacement boundary conditions (15) prescribed as formulated in Appendix 1 of [5] with an additional condition that the fibrous core is rigid and the binder shell is incompressible.

For the case where  $\beta$  is the same for all composite cylinders, an application of the upper bound theorem gives an upper bound  $\left(\tau_{23}^L\right)_U$  as a function of  $\beta$  and  $v_1$ :

$$\frac{\left(\tau_{23}^L\right)_U}{k} = 1 + v_1 (I_2 - 1) \quad (16)$$

where

$$I_2 = \frac{2}{\pi(1-\beta^2)^3} \int_{\beta}^1 \int_0^{2\pi} R \sqrt{\Phi(\beta, R) + \Psi(\beta, R) \cos \theta} d\theta dR \quad (17)$$

and

$$\begin{aligned} \Phi(\beta, R) &= \frac{\beta^4}{R^4} \left[ (\beta^4 + \beta^2 + 1) - \frac{3}{2} (\beta^2 + 1) \frac{\beta^2}{R^2} \right]^2 + \left[ -\frac{(4\beta^4 + \beta^2 + 1)}{2} + 3\beta^2 R^2 \right]^2 \\ \Psi(\beta, R) &= \frac{2\beta^2}{R^2} \left[ (\beta^4 + \beta^2 + 1) - \frac{3}{2} (\beta^2 + 1) \frac{\beta^2}{R^2} \right] \left[ -\frac{(4\beta^4 + \beta^2 + 1)}{2} + 3\beta^2 R^2 \right] \end{aligned} \quad (18)$$

In the case of "random array", (16) reduces to

$$\left( \frac{\tau_{23}^L}{k} \right)_U = I_2 \quad (19)$$

In Fig. 8,  $\left( \frac{\tau_{23}^L}{k} \right)_U$  in (19) is plotted as a function of  $v_f$  which shows that

$$\lim_{v_f \rightarrow 0} \left( \frac{\tau_{23}^L}{k} \right)_U = 1$$

and

$$\lim_{v_f \rightarrow 1} \left( \frac{\tau_{23}^L}{k} \right)_U = \infty$$

From the above result, it is seen that the upper and lower bounds for the limit load  $\tau_{23}^L$  are much farther apart than those for  $\tau_{12}^L$  in Case 1. Therefore, it is possible that the transverse shear strength of the specimen could be increased substantially by fiber-reinforcement. Further effort should be made to get closer bounds in order to have a better estimate of the limit load.

Case 3. Under the conditions of plane strain, the surface tractions in

(4) are such that  $\tau_{ij}$  has the following form:

$$\tau_{ij} = \begin{bmatrix} \tau_{11} & 0 & 0 \\ 0 & \tau_{22} & 0 \\ 0 & 0 & 0 \end{bmatrix} \quad (20)$$

where  $\tau_{11}$  and  $\tau_{22}$  are constants. This amounts to uniform tensile stress  $\tau_{22}$  applied on the lateral boundary of the specimen as depicted diagrammatically in Fig. 9 in the  $x_2x_3$  plane. The tractions equivalent to uniform tensile stress on the terminal sections are used to maintain the conditions of plane strain.

Using the same principle, the lower bound for the limit load is

$$\left( \tau_{22}^L \right)_L = 2k$$

For upper bound construction, a kinematically admissible velocity field is chosen which is obtained from the one constructed in Case 2 through an orthogonal transformation such that

$$u_i = \mathcal{L}_{ij} u_j'$$

with

$$\mathcal{L}_{ij} = \begin{bmatrix} 0 & 0 & 0 \\ 0 & \frac{1}{\sqrt{2}} & \frac{1}{\sqrt{2}} \\ 0 & -\frac{1}{\sqrt{2}} & \frac{1}{\sqrt{2}} \end{bmatrix}$$

where  $u_j^i$  are velocity components used in Case 2 referred to an  $x^i$ -system. Then, after some manipulation, it turns out that

$$\left( \tau_{22}^L \right)_U = 2 \left( \tau_{23}^L \right)_U \quad (21)$$

where  $\left( \tau_{23}^L \right)_U$  is given in Case 2.

The selection of the velocity field is not unique and it remains to be determined if a lower upper bound can be found by choosing another admissible field. Although this uncertainty cannot be removed until the bounds are shown to be the best possible bounds for the geometry considered, it is of interest to note an additional result. Hashin [6] has suggested a velocity field within the composite cylinders of the form:

$$\begin{aligned} u_r &= \frac{\gamma_2}{2} \rho(r) \cos 2\theta \\ u_\theta &= -\frac{\gamma_2}{2} \Omega(r) \sin 2\theta \end{aligned} \quad r_f \leq r \leq r_b$$

For  $\rho(r)$  assumed as a cubic in  $r$ , numerical results show that this field yields a higher upper bound than that defined by Eqs. (19) and (21).

Case 4. Under the conditions of plane strain, the surface tractions in (4) are such that  $\tau_{ij}$  has the following form:

$$\tau_{ij} = \begin{bmatrix} \tau_{11} & 0 & 0 \\ 0 & \tau_{22} & 0 \\ 0 & 0 & \tau_{33} \end{bmatrix} \quad (\tau_{22} \neq \tau_{33}) \quad (22)$$

where the non-vanishing components of stresses are all constants. This amounts to uniform biaxial uniform tensile stresses  $\tau_{22}$  and  $\tau_{33}$  applied on the lateral boundary of the specimen, under the conditions of plane strain, as depicted diagrammatically in Fig. 10.

For definiteness, assume  $\tau_{22} > \tau_{33}$ . Then following the ideas used in Case 3, it can be shown that

$$\left( \tau_{22} \right)_L - \left( \tau_{33} \right)_L = 2k$$

$$\text{and } \left( \tau_{22}^L \right)_U - \left( \tau_{33}^L \right)_U = 2 \left( \tau_{23}^L \right)_U$$

where  $\left( \tau_{23}^L \right)_U$  can be obtained from Case 2.

Case 5. The surface tractions in (4) are such that  $\tau_{ij}$  has the following

form:

$$\tau_{ij} = \begin{bmatrix} 0 & \tau_{12} & 0 \\ \tau_{12} & \tau_{22} & 0 \\ 0 & 0 & 0 \end{bmatrix} \quad (23)$$

where the constant stress components  $\tau_{12}$  and  $\tau_{22}$  are related in the following way:

$$\tau_{12} = \alpha \tau_{22} \quad (24)$$

with  $\alpha \geq 0$ . This amounts to a proportional loading of combined uniform shear stress  $\tau_{12}$  and uniform tensile stresses  $\tau_{22}$  on the boundary surface of the specimen as depicted diagrammatically in Figure 11 in the  $x_1 x_2$  plane.

Since both  $\tau_{12}$  and  $\tau_{22}$  are assumed finite, it is obvious that  $\alpha = 0$  corresponds to the case where only uniform tensile stresses  $\tau_{22}$  are present. On the other hand,  $\alpha \rightarrow \infty$  corresponds to the case where the specimen is subject only to uniform shear stresses  $\tau_{12}$ .

Lower bounds for  $\tau_{22}^L$  and  $\tau_{12}^L$  can be obtained easily:

$$\frac{\left( \tau_{22}^L \right)_L}{k} = \frac{1}{\sqrt{\frac{1}{3} + \alpha^2}} \quad (25)$$

and 
$$\left(\frac{\tau_{12}^L}{k}\right)_L = \frac{\alpha}{\sqrt{\frac{1}{3} + \alpha^2}}$$

for  $\alpha \geq 0$

For upper bound construction, a kinematically admissible velocity field  $\underline{u}$  is chosen to be a linear combination of the two kinematically admissible fields used in Case 1 and Case 3 with

$$\gamma_1 = \omega \gamma_2 \tag{26}$$

Equation (26) relates  $\gamma_1$  and  $\gamma_2$  which appears in (7) and (15), respectively.

Then an application of the upper bound theorem gives, for the case of constant  $\beta$  throughout the specimen.

$$\left(\frac{\tau_{22}^L}{k}\right)_U = \frac{\sqrt{1+\omega^2} + v_1 (I_3 - \sqrt{1+\omega^2})}{\frac{1}{2} + \alpha \omega} \tag{27}$$

where

$$I_3 = \frac{1}{\pi(1-\beta^2)^3} \int_{\beta}^1 \int_0^{2\pi} R \sqrt{\Phi_1(\omega, \beta, R) + \Phi_2(\omega, \beta, R) \cos \theta + \Phi_3(\beta, R) \cos 2\theta} d\theta dR$$

$$\Phi_1(\omega, \beta, R) = 4 \left\{ \frac{\beta^4}{R^4} \left[ (\beta^4 + \beta^2 + 1) - \frac{3}{2} (\beta^2 + 1) \frac{\beta^2}{R^2} \right]^2 + \left[ 3\beta^2 R^2 - \frac{(4\beta^4 + \beta^2 + 1)}{2} \right]^2 \right\} + \omega^2 (1-\beta^2)^4 \left( 1 + \frac{\beta^4}{R^4} \right)$$

$$\Phi_2(\omega, \beta, R) = 2 \omega^2 (1-\beta^2)^4 \frac{\beta^2}{R^2}$$

and

$$\Phi_3(\beta, R) = 8 \frac{\beta^2}{R^2} \left[ (\beta^4 + \beta^2 + 1) - \frac{3}{2} (\beta^2 + 1) \frac{\beta^2}{R^2} \right] \left[ 3 \beta^2 R^2 - \frac{(4\beta^4 + \beta^2 + 1)}{2} \right]$$

In the case of "random array", (27) reduces to

$$\left( \tau_{22}^L \right)_U = \frac{I_3}{\frac{1}{2} + \alpha \omega} \quad (28)$$

Since  $\omega$  in (26) is arbitrary, the lowest upper bound among the class of upper bounds in (28), will be obtained by minimizing the right hand side of (28) with respect to  $\omega$ . Thus,

$$\left( \tau_{22}^L \right)_U = \min_{\{ \omega \}} \frac{k I_3}{\frac{1}{2} + \alpha \omega} \quad (29)$$

and

$$\left( \tau_{12}^L \right)_U = \min_{\{ \omega \}} \frac{k \alpha I_3}{\frac{1}{2} + \alpha \omega}$$

will be chosen as the upper bounds for  $\tau_{22}^L$  and  $\tau_{12}^L$ , respectively.

Numerical calculation is performed to obtain  $\left( \tau_{22}^L \right)_U$  and  $\left( \tau_{12}^L \right)_U$  from (29) for different values of  $\beta$  and  $\alpha$ . It is interesting to note that in the numerical calculation, for any given  $\beta$ ,  $\omega$  which minimizes the right hand side of equation (29) is a monotonic increasing function of  $\alpha$  but  $\omega \neq \alpha$  (except when  $\alpha = 0$ , then  $\omega = \alpha = 0$ ). The results are summarized in Figure 12 in which  $\beta^2 = 0.8$  is the highest fiber volume fraction shown. The dotted curve represents (25) which gives the lower bound for  $\tau_{22}^L$  and  $\tau_{12}^L$  for any  $\beta$ .



## CONCLUSIONS

Bounds on the limit loads of uniaxial fibrous composites subjected to in-plane shear and transverse plane shear and extension stresses have been obtained. These results emphasize the strong influence of matrix properties upon composite strength. Interaction curves for the case of combined in-plane shear and transverse extension stresses were also obtained. This is a state of stress which has an important influence upon the strength of many composite laminates.

Further effort is indicated to obtain closer bounds on the limit load for certain cases. Further effort is also indicated for the development of composites utilizing matrix materials of higher strength.

## BIBLIOGRAPHY

1. Rosen, B. W., "Mechanics of Composite Strengthening", in "Fiber Composite Materials" published by American Society for Metals, Metals Park, Ohio, 1965.
2. Hashin, Z., "Transverse Strength of Fibrous Composites" in "Evaluation of Filament-Reinforced Composites for Aerospace Structural Applications", (Annual Report NASw-817) by Dow, N. F. and Rosen, B. W., October 26, 1964 .
3. Drucker, D. C., Greenberg, H. J. and Prager, W., "The Safety Factor of an Elastic-Plastic Body in Plane Strain", J. of Applied Mechanics, 18, pp. 371-378, 1951 b.
4. Koiter, W. T., "General Theorems for Elastic-Plastic Solids", Chapter IV in "Progress in Solid Mechanics", Sneddon and Hill, Eds., North Holland, 1960.
5. Hashin, Z. and Rosen, B. W., "The Elastic Moduli of Fiber-Reinforced Materials", J. of Applied Mechanics, Vol. 31E, pp. 223-232, June 1964.
6. Hashin, Z., Personal communication.

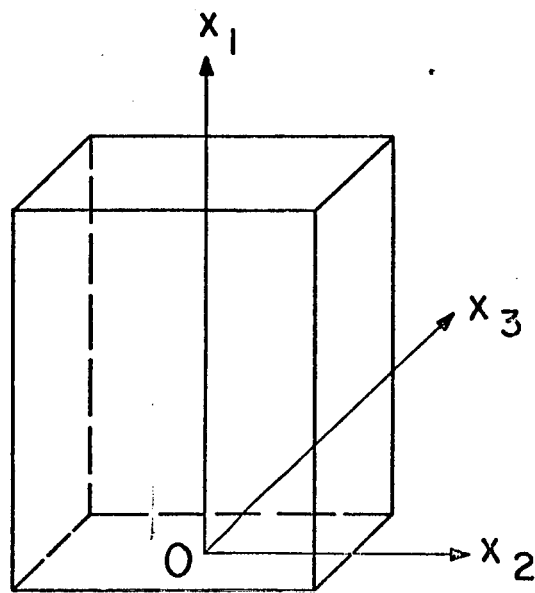


FIG. 1. COMPOSITE SPECIMEN  
( FIBERS IN  $x_1$  DIRECTION)

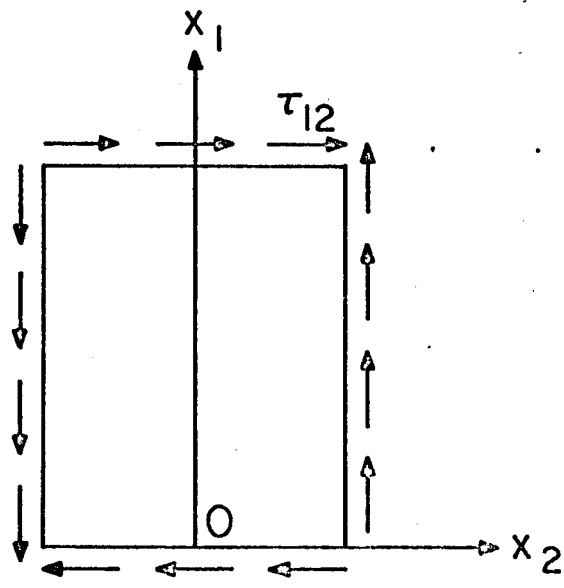


FIG. 2 - IN-PLANE SHEAR

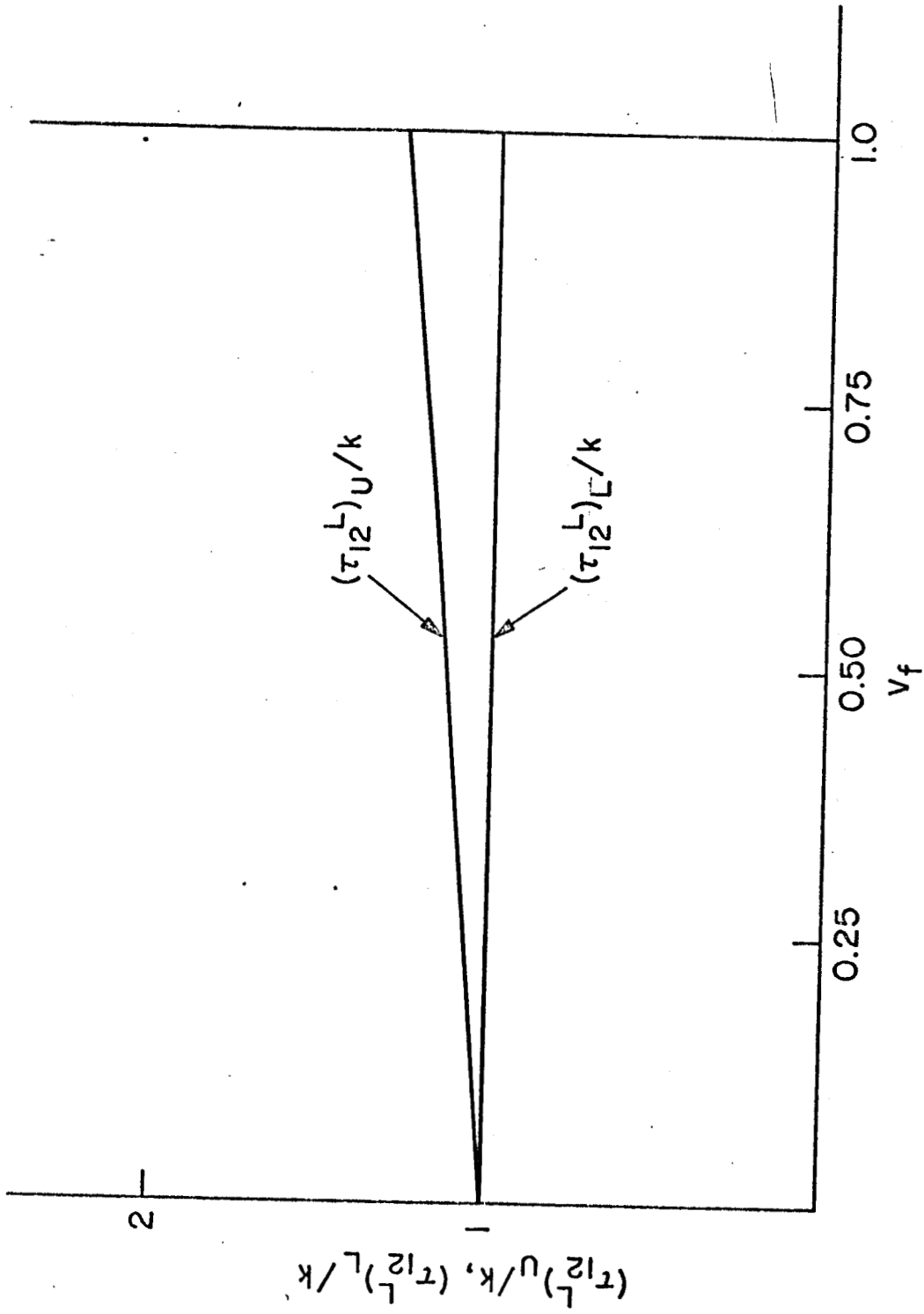


FIG. 3. - UPPER AND LOWER BOUNDS FOR  $\tau_{12}^L$ .

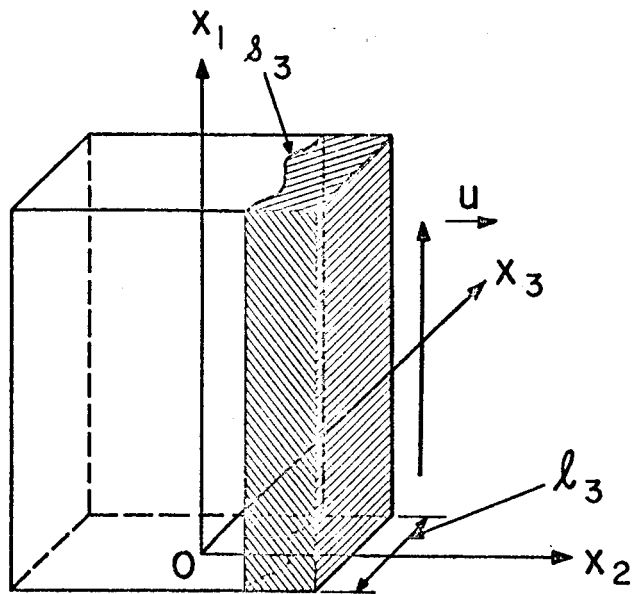


FIG. 4. - FIBERS IN  $x_1$  DIRECTION.

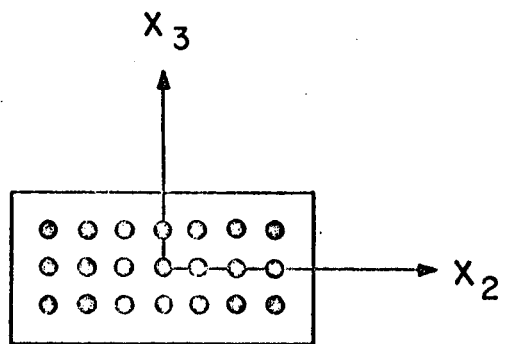


FIG. 5. - "SQUARE ARRAY"

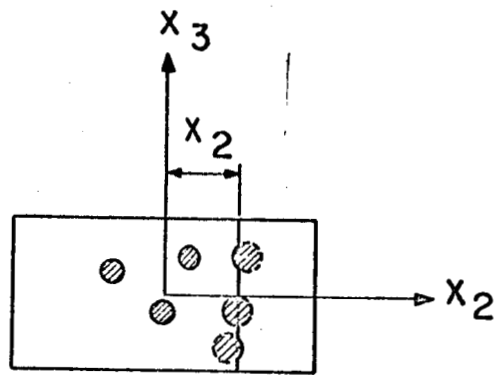


FIG. 6 - A TYPICAL CUT AT  $x_2$



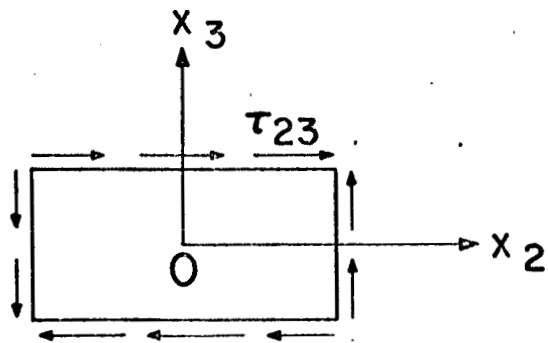


FIG. 7. - TRANSVERSE SHEAR  
(FIBERS PERPENDICULAR TO  $x_2$   $x_3$  PLANE)

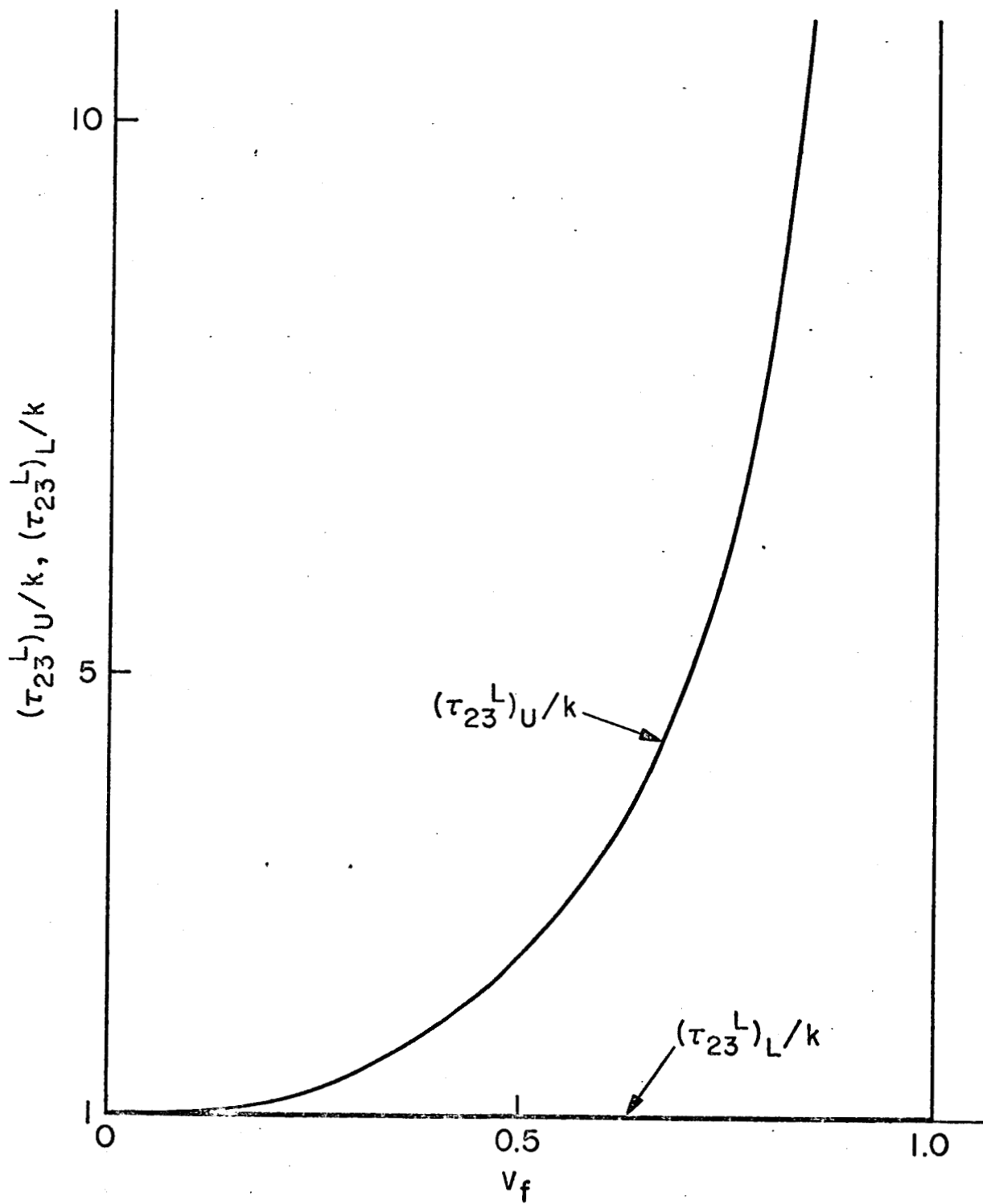


FIG. 8 - UPPER AND LOWER BOUNDS FOR  $\tau_{23}^L$ .

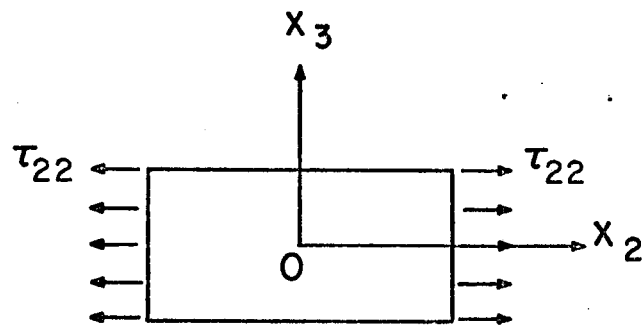


FIG. 9 - TRANSVERSE TENSION

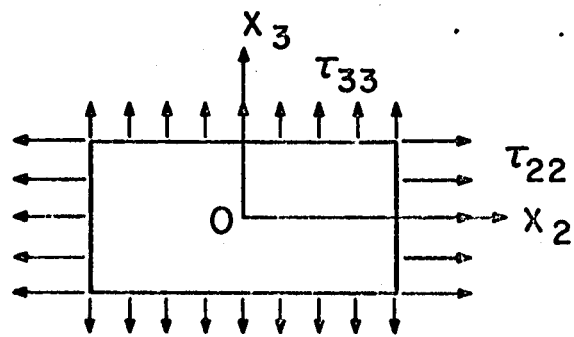


FIG. 10. - TRANSVERSE BIAXIAL TENSION

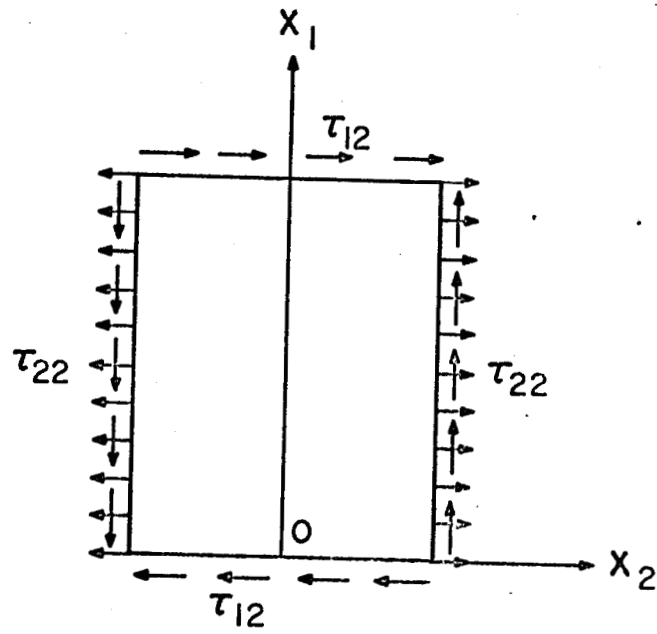


FIG. 11 - COMBINED STRESSES

$\frac{(\tau_{12}^L)_L}{k}$  VS.  $\frac{(\tau_{22}^L)_L}{k}$ , FOR ALL  $\beta^2 (0 < \beta^2 < 1)$

$\frac{(\tau_{12}^L)_U}{k}$  VS.  $\frac{(\tau_{22}^L)_U}{k}$

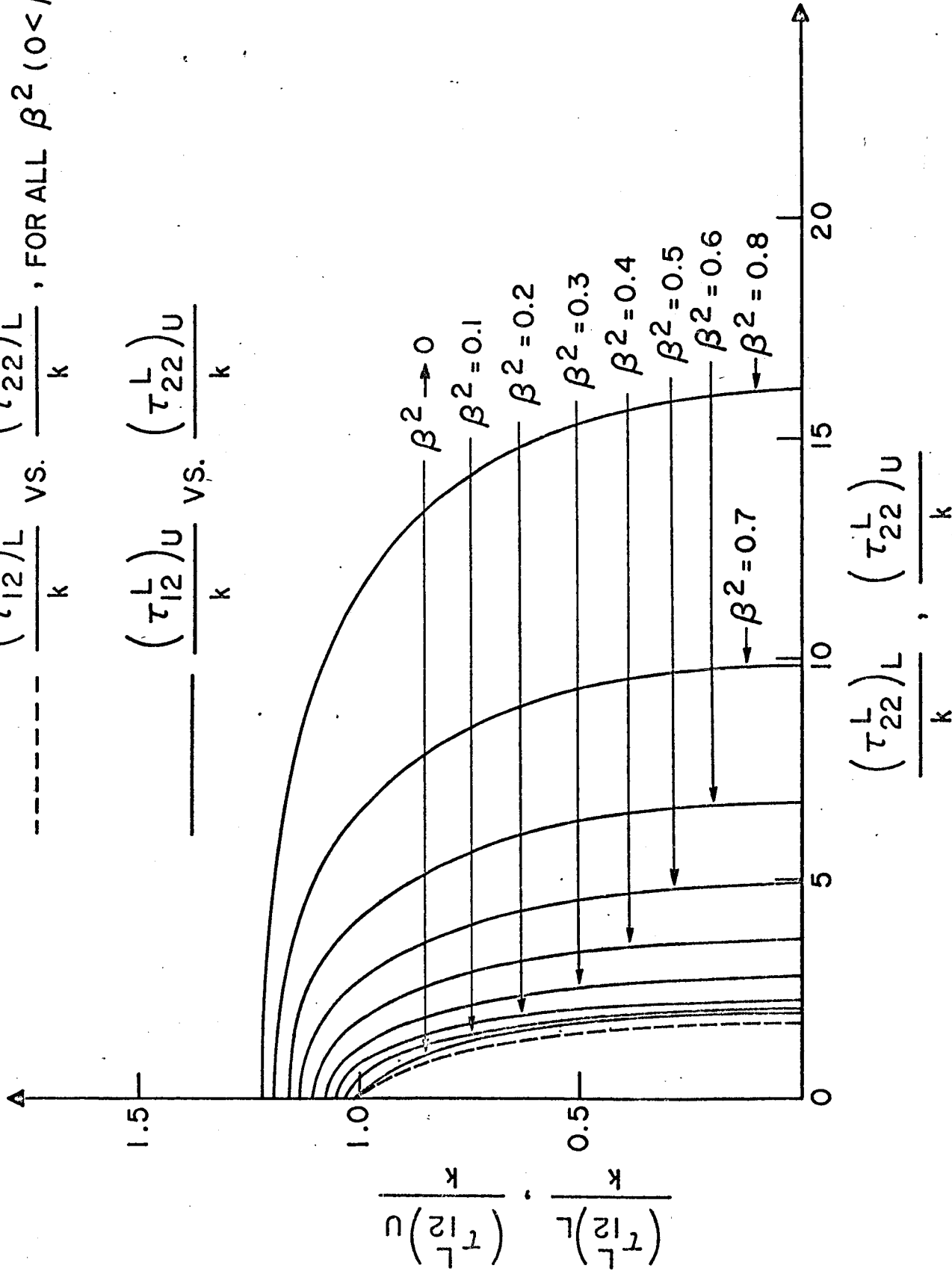


FIG. 12 - INTERACTION CURVES FOR COMBINED IN-PLANE SHEAR AND TRANSVERSE TENSION.